JOURNAL OF AGRICULTURAL AND FOOD CHEMISTRY
ARTICLE

J. Agric. Food Chem. 2011, 59, 481–490 481
DOI:10.1021/jf102917v

Alkyl and Other Major Structures in ^{13}C-Labeled Glucose-Glycine Melanoidins Identified by Solid-State Nuclear Magnetic Resonance

Xiaowen Fang and Klaus Schmidt-Rohr*

Department of Chemistry, Iowa State University, Ames, Iowa 50011, United States

The high molecular weight fraction of melanoidins formed in the Maillard reaction between isotopically labeled glucose and glycine has been characterized comprehensively using advanced ^{13}C and ^{15}N solid-state NMR with spectral editing. We have focused on the fate of glucose in a 1:1 molar ratio with glycine, heated as a coprecipitated powder at 125 °C for 2 h. Quantitative ^{13}C NMR spectra show that aromatic and alkene carbons make up only 40% of the total in the melanoidin. Spectra of melanoidins made from specifically labeled (^{13}C1, ^{13}C2, ^{13}C3, and ^{13}C6) glucose are strikingly different, proving that specific structures of various types are formed. More than half of the glucose-C1 carbons form new C−C bonds, not just C−O and C−N bonds. Most C2 carbons are bonded to N or O and not protonated, while C3 shows the reverse trends. C4 and C5 remain significantly in alkyl OCH sites or become part of heterocyclic aromatic rings. C6 undergoes the least transformation, remaining half in OCH_2 groups. Functional groups characteristic of fragmentation are relatively insignificant, except for N/O−C2═O groups indicating some $C_1 + C_5$ and $C_2 + C_4$ fragmentation. On the basis of ^{13}C−^{13}C and ^{15}N−^{13}C correlation spectra, 11 "monomer units" have been identified, including several types of alkyl chain or ring segments, furans, pyrroles, imidazoles, and oxazoles; these are mixed on the nanometer scale. This complexity explains why simple models cannot represent the structure of melanoidins. While none of the "monomer units" represents more than 15% of all C, the 11 units identified together account for more than half of all glucose carbon in the melanoidin.

KEYWORDS: Maillard reaction; solid-state NMR; spectral editing; furan; melanoidin models; COST action 919

INTRODUCTION

The Maillard reaction between reducing sugars and amine compounds is of importance in food, health, and environmental sciences (*1*−*6*). Its products are responsible for food aroma, browning color, and mutagenic properties. As a potential pathway of forming soil organic matter, the Maillard reaction may also play a role in the environment (*7*). The Maillard reaction is not a single chemical reaction but a complex reaction network (*1*, *2*, *4*, *5*). It has been shown that model Maillard reaction systems can be used to simulate the reactions occurring in food and in the human body (*2*). A general scheme proposed by Hodge in 1953 (*1*) and elaborated by many scientists (*2*, *4*, *5*) has been widely accepted. Because of the heterogeneity especially of the melanoidins, the high molecular weight (HMW) products, determination of their structure is challenging.

Most studies of the Maillard reaction have focused on the early stage products or dealt with small molecules (less than 1 kDa) (*4*, *8*−*10*), which account for <25% of Maillard products (*11*). Relatively little is known about the soluble HMW and the insoluble fraction, which account for most of the products under certain reaction conditions (*11*). Cämmerer and Kroh reported that the elemental composition of melanoidins is little affected by a change of the sugar:amine ratio from 4:1 to 1:1 and proposed a structure (*12*) with a bond between C1 and N of the otherwise unmodified amino acid, a double bond between C1−C2 or C2−C3, some C3 in CH_2 groups, and no change in C4, C5, and C6 (*12*). Other models also discounted the presence of pyrroles and instead proposed enamine- or imine-based structures (*13*, *14*). A very different model of melanoidins has been proposed by Tressl et al., containing mostly aromatic rings made from the polycondensation between N-substituted pyrroles, 2-furaldehyde, and N-substituted 2-formylpyrroles, connected mostly by one-carbon alkyl linkers (*4*).

The most comprehensive information on melanoidin structure has been provided by ^{13}C and ^{15}N nuclear magnetic resonance (NMR) studies (*15*−*20*). While these have shown evidence of the presence of furans and pyrroles, a detailed analysis of the transformations of glucose was prevented by strong peak overlap in the complex ^{13}C NMR spectra obtained.

In the present work, we have expanded the structural information on melanoidins provided by NMR, by applying a full complement of advanced solid-state NMR techniques to melanoidins made from ^{13}C-labeled glucose and ^{15}N-glycine. Quantitative

*To whom correspondence should be addressed. Tel: 515-294-6105. Fax: 515-294-0105. E-mail: srohr@iastate.edu.

Published on Web 12/28/2010

^{13}C NMR combined with spectral editing of signals from CH, CH_2, C−N, C- -N, alkyl C, and nonprotonated C provides detailed information on the functional groups formed and enables us to identify changes in the bonding of glucose carbons. The specific ^{13}C labeling of glucose allows us to trace the origins of carbons in the final products. Two-dimensional (2D) ^{15}N−^{13}C and ^{13}C−^{13}C experiments provide N−C and C−C connectivities that enable identification of a dozen common "monomer units" of the melanoidin. Two-dimensional ^{1}H−^{13}C experiments with ^{1}H spin diffusion are used to determine whether alkyl and aromatic components are mixed on the nanometer scale. We also show how spectral editing and 2D exchange spectroscopy enable identification of fragmentation products. Specifically, we have studied the soluble HMW and insoluble main products of the Maillard reaction, in dry conditions, between coprecipitated ^{13}C-glucose and ^{15}N-glycine. Samples have been prepared according to COST Action 919 (European COoperation in the field of Scientific and Technical research) (*5*, *21*−*23*). We have previously studied the fate of glycine in this material (*20*) and are now focusing on the more complex transformations of glucose.

EXPERIMENTAL PROCEDURES

Materials. D-Glucose, anhydrous 99+% (MW 180.16), and glycine, 98% (FW 75.06), were purchased from Acros Organics (NJ). D-Glucose with different ^{13}C-labeled sites, -$^{13}C_6$, -1-^{13}C, -2-^{13}C, -3-^{13}C, -6-^{13}C (all 99%), and glycine (-^{15}N, 98%), was selected based on availability and price and was obtained from Cambridge Isotope Laboratories (MA). D-Gglucose (-1,2-$^{13}C_2$, 99%) was obtained from Isotec (OH). Dialysis tubing made from regenerated cellulose, purchased from Fisherbrand, had a nominal MWCO of 6000−8000 Da and a volume/length of 5.10 mL/cm. Filter papers were 41 ashless from Whatman (England). Water was E-pure water (Barnstead).

Sample Preparation in the Dry Reaction Condition. Following refs *5* and *21*, an equimolar coprecipitated mixture of glucose and glycine was heated for 2 h at 125 °C. Filter papers were used to separate the insoluble fraction from the soluble fractions. After dialysis, the soluble HMW fraction of melanoidin was collected. Both the soluble HMW fraction and the insoluble fraction were used in this study. More details are given in ref *20*.

NMR Parameters. The NMR experiments were performed using a Bruker DSX400 spectrometer at 400 MHz for ^{1}H, 100 MHz for ^{13}C, and 40 MHz for ^{15}N. A Bruker 4 mm triple-resonance magic-angle spinning (MAS) probe head was used for measurements of ^{13}C- and ^{15}N-labeled samples at MAS speeds between 5 and 14 kHz, while unlabeled melanoidin samples were measured using a 7 mm Bruker double-resonance probe head at 6.5 kHz MAS. ^{13}C and ^{1}H chemical shifts were referenced to tetramethylsilane, using the COO resonance of glycine at 176.49 ppm and the proton resonance of hydroxyapatite at 0.18 ppm as secondary references. ^{15}N chemical shifts were indirectly referenced to liquid ammonia by setting the signal of *N*-acetyl-D-valine to 122 ppm. The 90° pulse lengths were 4 μs for both ^{13}C and ^{1}H and 6 μs for ^{15}N.

Cross-Polarization (CP)/Total Suppression of Sidebands (TOSS) NMR Experiments. For routine ^{13}C NMR characterization of various unlabeled and ^{13}C-labeled melanoidins, ^{13}C−CP spectra after four-pulse TOSS (*24*) were acquired at 6.5 kHz MAS, with a recycle delay of 3 s and CP contact time of 1 ms. Two-pulse phase modulation (TPPM) decoupling was applied during detection.

High-Speed Quantitative ^{13}C Direct-Polarization (DP)/Echo/MAS NMR. To quantitatively account for the contributions of the various, C1−C6, glucose carbons to the melanoidins, quantitative ^{13}C DP/Hahn echo/MAS NMR spectra were acquired for the samples made by reacting glucose-$^{13}C_6$, -^{13}C1, -^{13}C2, -^{13}C3, or -^{13}C6 with glycine-^{15}N, at 14 kHz MAS. The Hahn echo was used to avoid baseline distortion, and TPPM decoupling was applied during detection. The recycle delays were estimated by measuring CP/T_1 spectra with two or three $T_{1,C}$ filter times. The $T_{1,C}$ filter time for which the residual carbon signals were less than 5% was set as the recycle delay of the corresponding quantitative DP/MAS experiments, which ensures that all carbon sites are fully relaxed (*25*).

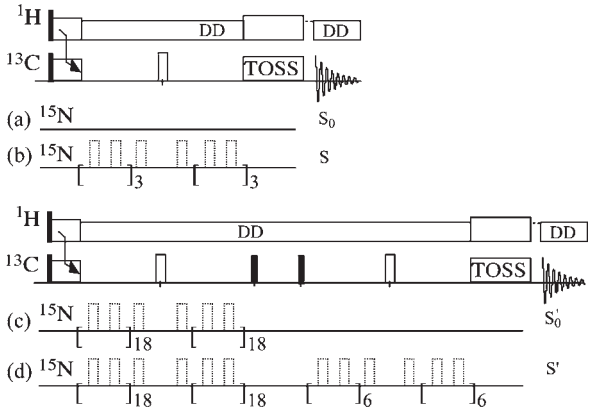

Figure 1. ^{13}C{^{15}N} REDOR pulse sequences for observing the signals of carbons near N and selectively observing the signals of carbons one or two bonds from their adjacent ^{15}N. Filled boxes represent 90° pulses. (**a**) Pulse sequence used to obtain the reference signal S_0 of all carbons. (**b**) Pulse sequence for recording the signal S of carbons not bonded to ^{15}N. (**c**) Reference pulse sequence used to obtain the signal S_0' of carbons within two bonds from ^{15}N (C−C−N). The 180° pulses on the ^{15}N channel are switched on and off, and the phase of the receiver is correspondingly alternated by 180° to subtract out the signals of carbons beyond a two-bond distance to ^{15}N. (**d**) Pulse sequence used to obtain the signals S′ of carbons two bonds from ^{15}N by an additional short ^{13}C{^{15}N} REDOR that dephases the signals of C directly bonded to N. The spectrum of those C−N carbons can be obtained by taking the difference between the two spectra.

The recycle delays were between 100 and 220 s, and the numbers of scans were between 32 and 128.

Background signals of ^{13}C in natural abundance (1.1% of all C) account for 8% of the spectral intensity in the melanoidins made from glucose with one ^{13}C-labeled site. This interference was removed from the DP/MAS spectra by subtracting the background spectrum (only of glycine for the $^{13}C_6$ sample), taking sample mass differences into account. Long T_{1C} relaxation times made it impractical to obtain the background spectrum by DP/MAS NMR of an unlabeled sample, and the CP/MAS spectrum underrepresents the signals of nonprotonated aromatic carbons. Instead, we generated the background spectrum with an excellent signal-to-noise ratio (and in semiquantitative agreement with the CP/MAS spectrum) as the sum of the DP/MAS spectra of the melanoidins made from uniformly ^{13}C-labeled glucose and from uniformly ^{13}C-labeled glycine, scaled down by the natural abundance factor of 0.011. The background correction does not change the visual appearance of the spectra significantly but results in more accurate quantitative data, for instance of the fractions of the various glucose carbons in the melanoidins.

CH and CH_2 Spectral Editing. CH (methine) signals can be selectively observed in dipolar distortionless enhancement by polarization experiments based on CH group multiple-quantum coherence not being dephased by the spin-pair CH dipolar coupling, while CH_2 group coherence is dephased by the dipolar coupling of the carbon to the second proton (*26*). Residual signals of nonprotonated C and CH_3 groups can be subtracted out by acquiring a second spectrum under the same conditions but additionally applying 40 μs of gated decoupling (dipolar dephasing) before detection. Spectral editing of CH_2 signals was achieved by selection of the three-spin coherence of CH_2 groups, using a ^{13}C 90° pulse and ^{1}H 0°/180° pulses applied after a quarter rotation period of MREV-8 decoupling (*27*). Any periods with z-magnetization were kept as short as possible, to avoid effects of ^{13}C spin exchange. The spinning speed was 5.787 kHz.

^{13}C Chemical Shift Anisotropy (CSA) Filter. Selective spectra of alkyl (sp^3-hybridized) carbons were obtained by the ^{13}C CSA filter technique (*28*, *29*) with three 180° pulses (plus two 90° pulses) and a filter time of 38 μs, which dephases the signals of sp^2- (and sp-) hybridized carbons by the recoupled CSA (*30*). During detection, TPPM decoupling was applied. The spinning speed was 6.5 kHz.

Selection of Carbons Near ^{15}N. To obtain semiquantitative information about the distribution of carbons that are within two bonds from ^{15}N, the ^{13}C{^{15}N} REDOR pulse sequences as shown in **Figure 1a**,**b** were

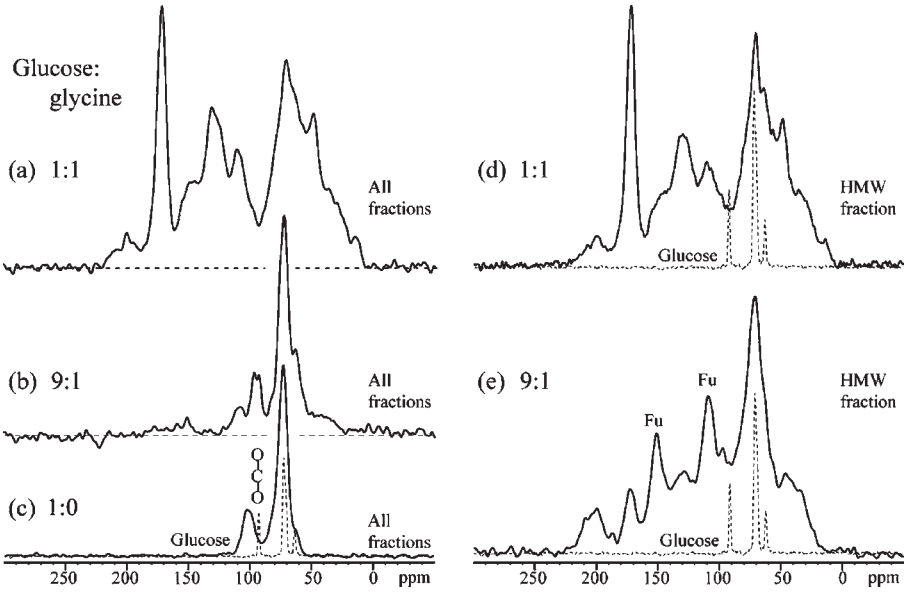

Figure 2. Cross-polarization ^{13}C NMR spectra of melanoidins prepared from glucose and glycine in a (**a**) 1:1 or (**b**) 9:1 ratio. (**c**) Neat glucose subjected to the same heating cycle as the reactants in panels **a** and **b**. (**d** and **e**) HMW fraction of the 1:1 and 9:1 melanoidin, respectively. Furan peaks are labeled "Fu". Thin dashed lines: spectrum of glucose, with three sharp peaks.

applied to HMW fraction melanoidins with selective glucose-^{13}C and glycine-^{15}N isotopic labeling. In this experiment, S gives signals of ^{13}C carbons that are two or more bonds away from ^{15}N, while S_0 is the corresponding CP spectrum of all ^{13}C carbons. The difference $\Delta S = S_0 - S$ is the spectrum of the carbons directly bonded to ^{15}N. A spinning frequency of 5 kHz and $N = 8$ rotation periods ($Nt_r = 1.6$ ms) were used.

To selectively observe the glucose carbons directly bonded to N (denoted as C−N) or two-bond from N (C- -N), a novel $^{13}C\{^{15}N\}$ medium and long distance (MELODI) (*31*) technique has been implemented. The pulse sequence shown in **Figure 1c** provides the signal S_0' of carbons within a one- or two-bond distance from N ("C−C−N"), by switching the 180° pulses on the ^{15}N channel on and off and inverting the receiver phase in alternating scans. This REDOR difference or heteronuclear coherence pulse sequence generates signals of carbons with dipolar couplings to ^{15}N. The longer the REDOR period, the longer the internuclear distances involved. Here, we used 38 rotation periods ($Nt_r = 5.6$ ms) at the MAS frequency of 7 kHz to recouple one- and two-bond C−N interactions. In the S' measurement, a second shorter REDOR period of 14 $t_r = 2$ ms duration was added, see **Figure 1d**, which selectively dephases the magnetization of N-bonded carbons ("C−N") due to their stronger dipolar coupling. Thus, only the signal S' of the carbons at a two-bond distance from the N ("C- -N") is retained. The difference $\Delta S' = S_0' - S'$ is the spectrum of carbons directly bonded to N ("C−N").

Two-Dimensional $^{15}N-^{13}C$ HSQC NMR. To detect the connectivities between glucose-^{13}C and glycine-^{15}N in the Maillard reaction products, the 2D $^{15}N-^{13}C$ heteronuclear single quantum (HSQC) pulse sequence (*32*) with REDOR recoupling was applied. The MAS frequency was 7 kHz, and the total experiment time was ca. 10 h per 2D spectrum.

Two-Dimensional $^{13}C-^{13}C$ Spin Exchange. The $^{13}C-^{13}C$ connectivities in the glucose-$^{13}C_6$ and glucose-1,2-^{13}C reaction samples were traced by 2D ^{13}C spin exchange experiments, with mixing times of 50 and 10 ms, respectively, to detect mostly cross-peaks between directly bonded carbons. TOSS-deTOSS, with four suitably spaced 180° pulses before and four after the evolution time t_1 (*33*), was used to remove spinning sidebands in the ω_1 dimension. A zero-frequency artifact at $\omega_1 = 0$ due to z-magnetization during t_1 was removed by a 90° phase shift of the last 180° pulse before t_1 coupled with a 180° shift of the receiver phase, in alternate scans. A third TOSS sequence was used before detection for spinning sideband suppression in the ω_2 dimension. A CP time of 1 ms and a MAS frequency of 7 kHz were used. The experiment was also performed with dipolar dephasing by gated decoupling before detection, which removes the signals of protonated carbons (except CH_3) in the ω_2 (horizontal) of the 2D spectrum and therefore about half of the cross-peaks. This enables more signal assignment, for example, to NCq (which overlaps with OCH) or to nonprotonated aromatic C. The number of remaining cross-peaks (0, 1, or 2) out of a pair is equal to the number of nonprotonated carbons in the pair. The experiment time was ca. 8 h per 2D spectrum.

Two-Dimensional $^{1}H-^{13}C$ NMR. Two-dimensional $^{1}H-^{13}C$ heteronuclear correlation (HetCor) NMR experiments with frequency-switched Lee−Goldburg homonuclear decoupling during the evolution time were performed at a spinning speed of 10 kHz. Lee−Goldburg cross-polarization (LG-CP) of 0.05 ms was used to suppress $^{1}H-^{1}H$ spin diffusion during polarization transfer and show mostly one-bond $^{1}H-^{13}C$ connectivity. A spin diffusion period of 0.45 ms was inserted before LG-CP to transfer ^{1}H magnetization on the 1 nm scale.

RESULTS AND DISCUSSION

Overall Spectra. CP/TOSS ^{13}C NMR spectra of melanoidins made from coprecipitated glucose and glycine in 1:1, 9:1, and 1:0 molar ratios are shown in **Figure 2a−c**. For comparison, the CP ^{13}C spectrum of glucose is also plotted in **Figure 2** (dashed thin lines). **Figure 2d,e** displays the CP spectra of the HMW fractions of melanoidins made from glucose and glycine in 1:1 or 9:1 ratios, respectively. The spectra confirm (*17*) that the Maillard reaction between glucose and glycine dramatically transforms the glucose structure. Before the reaction, glucose gives three sharp peaks at 93, 72, and 62 ppm, assigned to the anomeric O−CH−O (C1) carbon, the four CH−OH groups, and the CH_2−OH (C6) moiety, respectively. After the reaction, a wide variety of C═O, aromatic, O-alkyl, and nonpolar alkyl resonances are observed. For the 1:1 ratio, the spectrum of the HMW fraction in **Figure 2d** resembles that of the total melanoidin in **Figure 2a**. Thus, a study of the HMW fraction can capture the essential structural features of the total melanoidin. This is confirmed by spectral analysis of the insoluble fraction, which accounts for the majority of this material (*11*).

When the concentration of glucose is higher than that of glycine, in the 9:1 samples, there are more ketones (with signals between 220 and 185 ppm) and more furans with characteristic peaks at 150 and 110 ppm. The reduced concentration of nitrogen-containing heterocyclic aromatic compounds such as pyrrole (with peaks at 135 and 110 ppm) is not surprising, given the lower concentration of N in the reaction mixture. On the other hand, the relatively low concentration of furans in the 1:1 glucose: glycine melanoidin matches the reduction of furans by amines

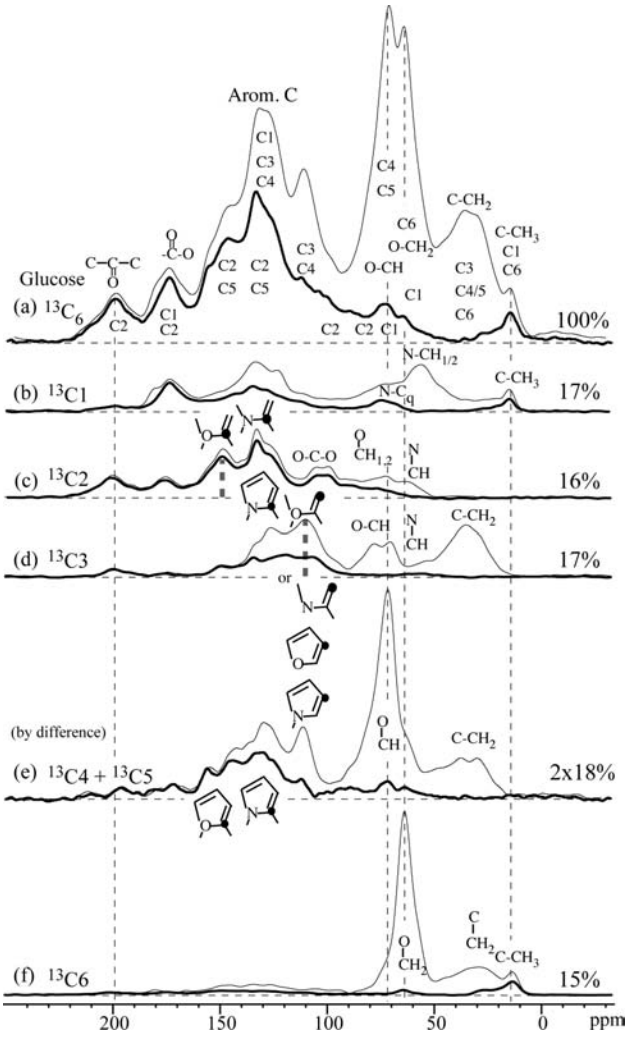

Figure 3. Quantitative direct polarization ^{13}C NMR spectra (thin lines) of soluble HMW melanoidins formed by reacting different ^{13}C-labeled ((**a**) $^{13}C_6$, (**b**) $^{13}C1$, (**c**) $^{13}C2$, (**d**) $^{13}C3$, and (**f**) $^{13}C6$) glucose with ^{15}N-labeled glycine in a 1:1 ratio. The spectrum in (**e**) was obtained by taking the difference between the glucose-$^{13}C_6$ spectrum and the sum spectrum of glucose-$^{13}C1$, -$^{13}C2$, -$^{13}C3$, and -$^{13}C6$. Thick lines: corresponding spectra of nonprotonated and methyl carbons selected by 68 μs of gated decoupling (dipolar dephasing) before detection.

reported in the literature (*2*). More −O−CH structures remain in the 9:1 melanoidin, as witnessed by the peak near 75 ppm in **Figure 2e**. In fact, the spectrum of the unfractionated reaction mixture, see **Figure 2b**, is completely dominated by −O−CH signals. Because the HMW melanoidin is apparently only a small fraction of the reaction mixture, we did not study this material in more detail.

Without glycine, dry heating of glucose at 125 °C for 2 h does not lead to major structural changes, as shown by its basically unchanged spectrum in **Figure 2c**, retaining the original three peaks, only broadened. The sugar has become amorphous or undergone oligomerization, without significant changes in the basic structure of the sugar rings. This demonstrates that in this solvent-free reaction, amine compounds play a crucial role in the transformation of sugar into more complex compounds.

Spectra of Each Glucose Carbon in the Melanoidin. Quantitative DP/Hahn echo/MAS ^{13}C NMR spectra of the soluble HMW melanoidin samples prepared from specifically ^{13}C-labeled glucose reacted with ^{15}N-labeled glycine are plotted in **Figure 3**. From top to bottom, the samples are glucose-$^{13}C_6$, -$^{13}C1$, -$^{13}C2$, -$^{13}C3$, and -$^{13}C6$. The intensity of each spectrum has been normalized per

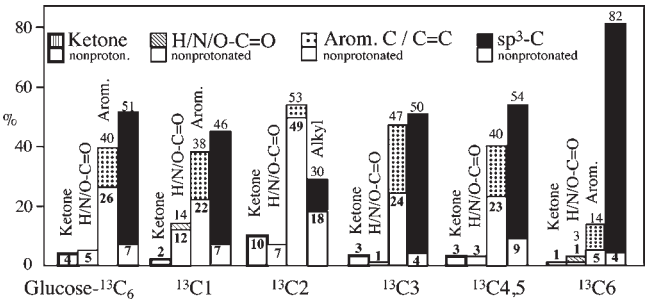

Figure 4. Percentages of various functional groups of each glucose carbon. The functional groups for each glucose carbon from left to right are ketones; carboxyl, amide, or aldehyde; aromatic or alkene carbons; and sp^3-hybridized (alkyl) carbons. The white bars are their corresponding nonprotonated carbon percentages (numbers in bold).

scan and mass of sample in the rotor, and the low natural abundance background has been removed. The spectrum of $^{13}C4$ plus $^{13}C5$ was obtained by subtracting the sum of the spectra of glucose-$^{13}C1$, -$^{13}C2$, -$^{13}C3$, and -$^{13}C6$ from the spectrum of glucose-$^{13}C_6$. The thin lines are the spectra of all types of carbons, while the thick lines trace the corresponding selective spectra of nonprotonated and CH_3 carbons. Corresponding spectra of the insoluble fraction are shown in Figure S1 in the Supporting Information.

The spectra in **Figure 3** show striking differences between the structures formed by different glucose carbons (C1−C6), proving that specific compounds are generated during the Maillard reaction without solvent. They can generally be divided into four relatively distinct spectral ranges: ketones resonating from 220 to 185 ppm, amide and COO carbons from 185 to 160 ppm, aromatic and other C=C carbons from 160 to 100 ppm, and alkyl carbons from 115 to 0 ppm. Setting the area of each spectrum to 100%, the percentages of these four subgroups are shown in **Figure 4**. C1−C5 of glucose produce significant amounts of both alkyl and aromatic carbons in the melanoidin, while C6 remains mostly in alkyl moieties. C=O carbons make up 4−17%. The data indicate that about 40% of all carbons are in aromatic rings or alkenes.

Advanced NMR with spectral editing can identify more than the four categories of functional groups shown in **Figure 4** and can also separate aromatic and *O*-alkyl resonances overlapping near 100 ppm. **Figure 5** shows spectral editing results for the melanoidins made by reacting glycine-^{15}N with glucose-$^{13}C1$ (**a**−**d**) or glucose-$^{13}C6$ (**e**−**h**). **Figure 5a**,**e** displays quantitative ^{13}C spectra (thin lines) and corresponding spectra of nonprotonated ^{13}C and $^{13}CH_3$ (thick lines). **Figure 5b**,**f** are selective spectra of the alkyl carbons and of the quaternary alkyls plus methyls, obtained by CSA filtering without or with dipolar dephasing (thin or thick lines, respectively). **Figure 5c**,**g** are the CH-only (thin line) and CH_2-only (thick line) spectra. **Figure 5d**,**h** show spectra of ^{13}C near ^{15}N, within one or two bonds from nitrogen (C−C−N, thin lines), directly bonded to nitrogen (C−N, thick lines), and two bonds from nitrogen (C- -N, dashed lines), obtained using the pulse sequence shown in **Figure 1**. **Figures 6** and **7** show analogous selective spectra of samples made from glucose-$^{13}C2$, -$^{13}C3$, and -$^{13}C_6$.

Insoluble vs HMW Fractions. The quantitative spectra of each glucose carbon in the insoluble fraction melanoidins in Figure S1 in the Supporting Information show similar spectral features and percentages as in the HMW fraction in **Figure 3**, with larger aromatic and smaller *O*-alkyl components in the insoluble fraction as the only significant differences. The results indicate that the structures of the insoluble fraction are distinguished mostly by a higher degree of polymerization or cross-linking, not by further

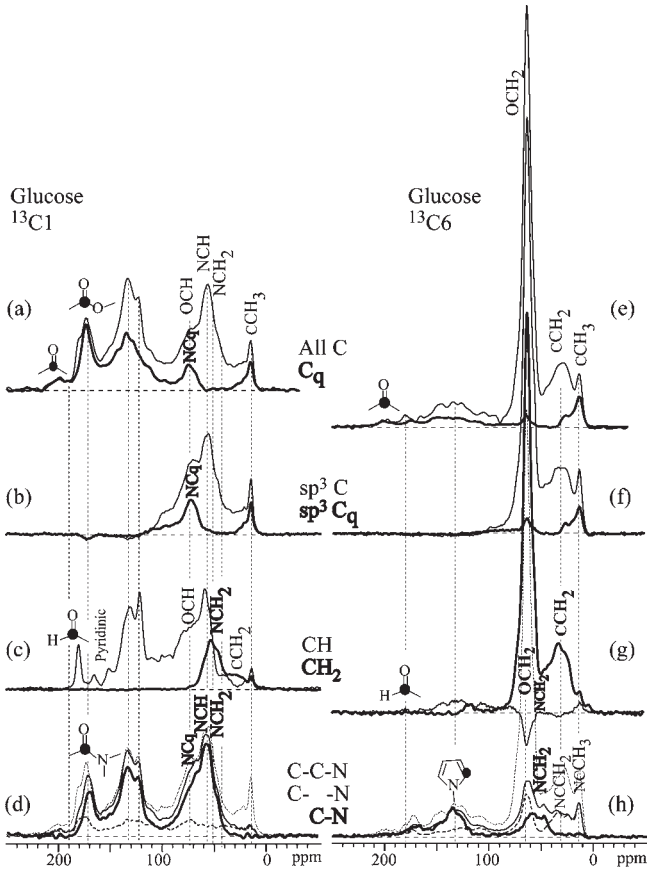

Figure 5. ^{13}C NMR spectral editing of soluble HMW melanoidins made from glucose-^{13}C1 or glucose-^{13}C6 reacted with glycine-^{15}N, plotted in panels **a**−**d** and **e**−**h**, respectively. (**a** and **e**) Thin lines: Quantitative spectrum of glucose-C1 or glucose-C6 in the products. Thick lines: Corresponding spectra of nonprotonated and methyl carbons after dipolar dephasing. (**b** and **f**) Thin lines: CSA-filtered spectra. Thick lines: Nonprotonated and methyl sp^3-hybridized ^{13}C. (**c** and **g**) Thin lines: CH-only spectra. Thick lines: CH_2-only, both with some CH_3 contributions. (**d** and **h**) Solid thin lines: Signals of carbons within two bonds from nitrogen. Thick lines: carbons directly bonded to nitrogen. Dashed lines: signal of carbons that are two bonds from nitrogen. Dashed thin lines: Full spectrum S_0 in ^{13}C{^{15}N} REDOR experiments; the corresponding ΔS spectrum virtually coincides with the thick line spectrum of ^{13}C bonded to N.

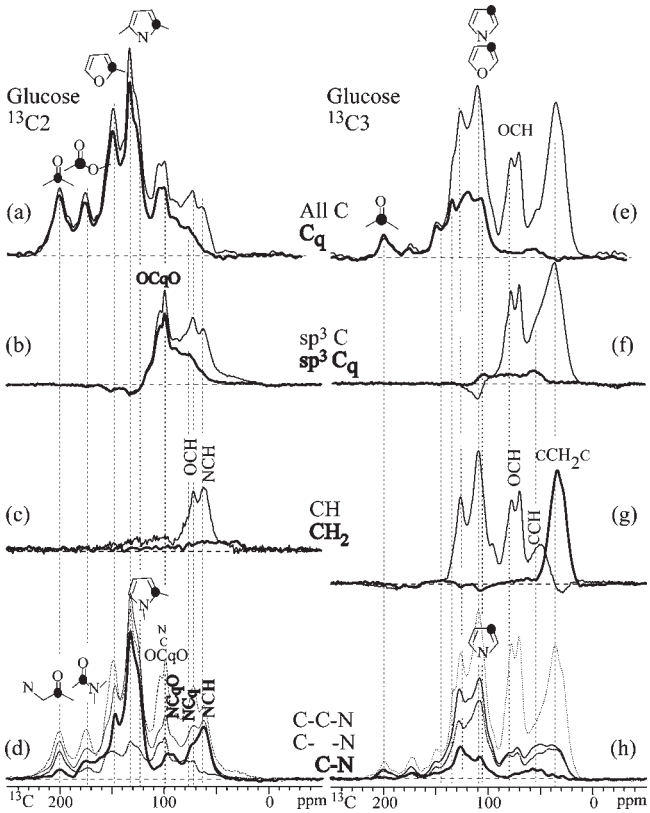

Figure 6. ^{13}C NMR spectral editing of soluble HMW melanoidins made from glucose-^{13}C2 or glucose-^{13}C3 reacted with glycine-^{15}N, plotted in panels **a**−**d** or **e**−**h**, respectively. The details of the plots are as described in the caption of **Figure 5**.

major chemical transformations. In the rest of this paper, we follow the COST Action 919 protocol in focusing on the soluble HMW fraction (*5*, *21*−*23*), to enable comparison of our results with those of other research groups.

Alkyl Fractions in Melanoidins. In the literature, for most volatile or low molecular weight compounds (*4*, *13*, *34*), and in various structural models of melanoidins (*4*, *23*), aromatic furan and/or pyrrole rings are often considered as the primary constituent units. Alkyl carbons have seldom been reported as the major units in melanoidins; Cämmerer's model (*12*) is a rare exception but still does not contain glucose C2 in alkyl sites. In our experiments, see **Figures 3** and **4**, we found that all glucose carbons produce alkyl structures in the melanoidin. Overall, alkyl carbons account for ∼51% of sugar carbons in melanoidins, and more than 85% of them are protonated. For obtaining accurate alkyl fractions, the overlap between alkyl and aromatic carbons between 115 and 100 ppm must be resolved, which was achieved by CSA filtering (see **Figures 5b**,**f**, **6b**,**f**, and **7b**).

Figure 4 shows that the alkyl carbon percentages of glucose-C3 and -C4,5 are similar, near 52%, while 82% of C6 are alkyl carbons. This indicates that C6 goes through the least transformation and that many of the alkyl C6H_2 and C6H_3 groups must be bonded to aromatic rings, since all other glucose carbons result in more aromatic structures. Given that most of the heterocyclic aromatic rings in melanoidins contain four carbon atoms, one or two carbons of glucose are available to form alkyl linkers or end groups. Thus, the aromatic fraction of ≤40% (this percentage includes alkenes, too) is associated with 10−20% of short alkyl segments, and the fraction of longer alkyl segments (and associated C=O groups) is 40−50%. The main features of the alkyl carbons are listed in detail in the Supporting Information.

sp^2 Hybridized Carbons in Melanoidin. According to **Figure 3a** and **Figure 4**, sp^2-hybridized carbons account for 49% of total sugar carbons. Aromatic and alkene carbons resonating between 160 and 100 ppm make up 40%. Various heterocyclic aromatic rings are formed in the melanoidin studied here, such as furan, pyrrole, imidazolium, and oxazolium; specific information on the nitrogen-containing rings can be obtained from 2D ^{15}N−^{13}C HSQC and 3D ^{15}N−^{13}C-^{13}C spectra to be discussed in a future publication. Carbonyl carbons (∼9%) are found in ketones resonating around 200 ppm, mainly from C2, with contributions from C3, 4/5, and in amides or carboxylates resonating around 175 ppm, mainly from C1 and C2. Small amounts of C1 formed aldehydes, HC=O, resonating at 180 ppm; see **Figure 5a**,**c**. Signals of C2 and C3 at 200 ppm could be due to a small amount of these carbons simultaneously double-bonded to oxygen to form 2,3-α-dicarbonyl compounds, which were found in Maillard reaction intermediates (*2*).

New C−C Bond Formation. In the original glucose molecules, C1 is bonded to only one carbon (i.e., C2). After the Maillard reaction, according to **Figure 3b** and **Figure 5a**−**d**, nonprotonated C1 between 150 and 20 ppm accounts for 29%, plus alkyl-CH for

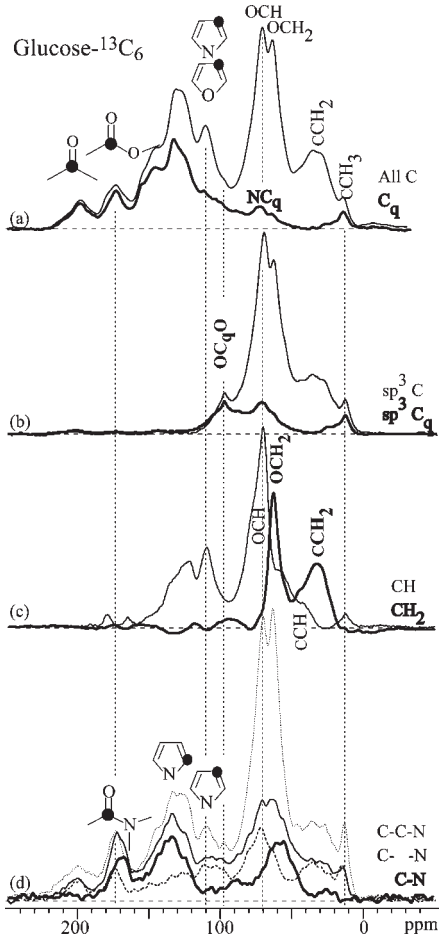

Figure 7. ^{13}C NMR spectral editing of soluble HMW melanoidins made from glucose-$^{13}C_6$ reacted with glycine-^{15}N, plotted in panels **a**−**d** or **e**−**h**, respectively. The details of the plots are as described in the caption of **Figure 5**.

20% and C−CH_2−C for 5% of total C1. In all of these structures, C1 is bonded to at least two carbons. Thus, about half of the C1 carbons of glucose must have formed additional (i.e., new) C−C bonds. At least some of these are likely linkages that help form HMW melanoidins. C6, as an end group carbon, is also prone to form some new C−C bonds, in C−CH_2−*C* units (16%) and aromatic rings (5% nonprotonated) but to a much smaller extent than C1. Analysis of the other glucose carbons shows an even lower level of additional bond formation. Thus, C1 of glucose stands out in its propensity for new C−C bond formation during the Maillard reaction.

C−N Bond Formation. From our previous study (*20*), it is clear that nitrogen of glycine is very reactive. After the Maillard reaction, the nitrogen has changed into various compounds with new chemical bonds with sugar carbons; see the bottom spectra of C bonded to N in **Figures 5**−**7**. The ^{13}C and ^{15}N labeling of the melanoidins enables us to apply 2D ^{15}N−^{13}C correlation spectroscopy to observe the carbon−nitrogen connectivities. **Figure 8** shows the 2D HSQC spectra of melanoidins made from different selectively ^{13}C-labeled glucoses reacted with ^{15}N-labeled glycine. From top to bottom, the melanoidins were prepared from glucose-$^{13}C_6$, glucose-$^{13}C1$, and -$^{13}C2$. **Figures 8d**−**f** show corresponding HSQC spectra of nonprotonated and methyl carbons only. CP/MAS ^{15}N NMR spectra of the three samples are shown along the vertical axes on the left of **Figure 8**; they show good reproducibility of the reaction. Projections of the spectra onto the ^{15}N axis are shown on the right. The strong ^{15}N signals near 120 ppm in **Figure 8b** shows that amide nitrogen is bonded mostly to C1. This includes alkyl C1 in (O=C)−N−C1H units, where the C=O carbon must be mostly provided by C1 and C2 from another glucose molecule, since glycine forms only a small fraction of amides (*20*).

Some nitrogen formed heterocyclic aromatic rings bonding to C1 and C2 but less to C3 and C6 (see **Figures 5**, **6**, and **8**). As a symmetric counterpart, C5 may also form C−N bonds in those aromatic rings. The near-absence of cross-peaks between aromatic C and amine N near the top center of the ^{15}N−^{13}C spectra in **Figure 8** shows that amine type nitrogens are rarely bonded to aromatic rings. An exception is seen prominently in the spectrum of the $^{13}C2$-labeled sample, **Figure 8c**,**f**, where a nonprotonated aromatic C (150 ppm) is bonded to amine N (62 ppm).

C−O Bond Cleavage and Formation. Condensation and dehydration make most C1, C2, C3, and some C4, C5, and C6 carbons lose hydroxyl groups, to form CCH_n, NCH_n, NC_q, and CCH_3, as well as some alkene carbons or nitrogen-containing aromatic rings. In addition to C−O bond cleavage, some new C−O bond formation also occurs, for instance when two furan carbons share one oxygen atom. In addition to O−C=O groups of several carbon sites, peaks of OC2O, with one alkyl carbon bonded to two oxygen atoms, are observed near 100 ppm in **Figure 6b**.

Fragmentation. C2, C3, C4, and C5 in glucose each have two C−C bonds. Fragmentation of the glucose backbone can be detected if these carbons end up in functional groups that have only one C−C bond. These moieties include COO and NC=O, O−C−H and N−C−H in furan and pyrrole rings, O−CH−O, NCH_2 and OCH_2, and all types of CH_3 groups. The spectra of **Figures 3**, **5**, and **6** show that of these, only COO and NC=O signals (at ∼175 ppm) exhibit significant intensity. The COO/NC=O signals are most intense for C2 (∼7% of C2). This indicates that fragmentation at C2, that is, either $C_1 + C_5$ or $C_2 + C_4$, is the most common (*4*). It is interesting to note that signals of isolated NCH_3 and OCH_3 glucose-derived carbons are completely absent. $C_1 + C_5$ fragmentation is also evidenced by the weak cross-peaks between aromatic C2 and alkyl C1 associated with furan and pyrrole rings in melanoidins made from $^{13}C1$-$^{13}C2$ glucose; see **Figure 9a**. Overall, we estimate that between 1/4 and 1/2 of all glucose carbon backbones are fragmented.

Specific Structural Fragments. The connectivities of the functional groups in larger structural fragments can be determined by analysis of cross-peaks in 2D ^{13}C spin exchange spectra as shown in **Figure 9**. **Figure 9a**,**b** shows spectra of melanoidin made from 50% diluted ^{13}C 1,2-labeled glucose, while those in **Figure 9c**,**d** are from $^{13}C_6$-labeled glucose. In **Figure 9b**,**d**, the signals of nonprotonated and methyl carbons were selected in the ω_2 dimension by 40 μs of dipolar dephasing. In the full spectra without dipolar dephasing, each pair of coupled ^{13}C spins shows two cross-peaks symmetrically on either side of the diagonal. In most cases, we have labeled only one of the two cross-peaks with capital letters, usually in the upper left half of the spectrum. In the following, several specific structures are proposed and listed in **Table 1**, with letters A−G matching the labels of the cross-peaks in **Figure 9**.

Quaternary O−C−O. Ketal (O−Cq−O) carbons resonating at ∼100 ppm are mainly from glucose C2, according to **Figure 3c**. A sharp cross-peak between this ketal carbon signal and the polar alkyl carbon (−O−C3H) at 70 ppm in **Figure 9c** can be clearly identified, telling us that the ketal C2 is bonded to C3 in an −O−CH group. Meanwhile, in **Figure 9a**, the ketal C2 carbon also shows a clear cross-peak with a protonated C1 carbon resonating at 54 ppm, assigned to −N−CH. The N in this structure is in an amide moiety (i.e., bonded to a C=O group), according to the HSQC spectrum of **Figure 8b**. Because the polar

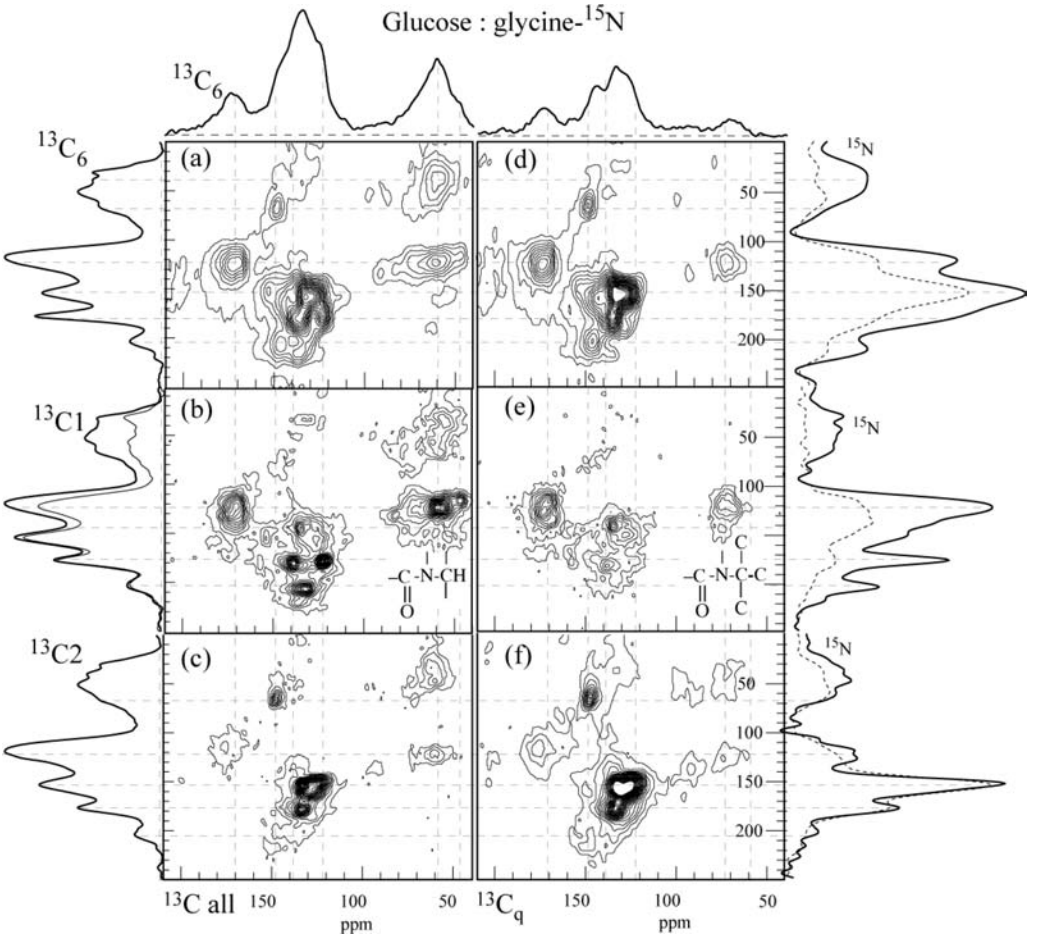

Figure 8. Two-dimensional $^{15}N-^{13}C$ HSQC NMR spectra of soluble HMW melanoidins made from selectively ^{13}C-labeled glucose reacted with ^{15}N-labeled glycine. From top to bottom, the sites of ^{13}C-labeled glucose are (**a** and **d**) -$^{13}C_6$, (**b** and **e**) -$^{13}C1$, and (**c** and **f**) -$^{13}C2$. The spectra on the right, panels **d**–**f**, were obtained after dipolar dephasing and show only signals of nonprotonated and methyl carbons. ^{15}N CP/MAS spectra of the three samples are shown on the left. Projections onto the ^{15}N dimension are shown on the right; continuous lines are for the left column without, dashed lines for the right column with $^{1}H-^{13}C$ dipolar dephasing.

alkyl carbons have prominent cross-peaks among themselves, seen in **Figure 9c**, we can propose structure A in **Table 1**, where C3 connects with the rest of the untransformed polar alkyl chain. The structure is shown cyclized into a saturated ring, which seems likely to avoid the presence of a geminal diol, which could convert into a ketone by loss of a water molecule. On the basis of the intensity of the NC1H and OC2qO peaks, this type of structure accounts for ca. 10% of all sugar C.

Ester or Amide C1 Carbon. The ester or amide C1 carbon resonating at 175 ppm, see **Figure 5d**, is bonded to a protonated polar alkyl C2 resonating at 60 ppm, according to one of the strongest cross-peaks in **Figure 9a**. From **Figure 6d**, we can see that most C2 resonating at 60 ppm is bonded to nitrogen as NC2H. Because the next carbon, C3, shows a strong resonance at 38 ppm of CH_2 two bonds from N, see **Figure 6g**/**h**, the strong cross-peak intensity at (60 and 38 ppm) in **Figure 9c** can be assigned to a $NC2H-C3H_2$ linkage. The additional strong cross-peak intensity at (70 and 38 ppm) could be due to a linkage between $C3H_2$ and the commonly occurring C4H–O segment. On that basis, structure B can be proposed, which for C3–C6 is the same as in some Maillard reaction intermediates (*4*) and in Cämmerer's model (*12*). On the basis of the intensity of the ester/amide C1 and NC2H peaks, it accounts for ca. 8% of all sugar C.

Aldehyde C1 Carbon. According to **Figure 9a**, the aldehyde (H–C=O) C1 carbon resonating at 181 ppm is bonded to a nonprotonated aromatic C2 resonating at 132 ppm. The aldehyde C1 carbon is two bonds from N, as seen in **Figure 5d**, and C2 is directly bonded to N, as seen in **Figure 6d**, confirming that the aromatic ring is a pyrrole. Therefore the structure C can be proposed. The C6 could be CH_3 or OCH_2 since both candidates are supported by cross-peaks in **Figure 9c**. This structure accounts for ca. 1.5% of all C.

Acetyl Groups. Amide or ester carbons resonating at 178 ppm also show a cross-peak with methyl resonances at 14 ppm in **Figure 9a**, where the methyl carbon is from C1 and the amide or ester carbon from C2. Because $C1H_3$ is more than two bonds from N, see **Figure 5d**, the C2 carbon must be an ester; see structure D in **Table 1**. These acetyl groups must have been formed by $C_2 + C_4$ fragmentation (*4*) and account for ca. 1% of all C.

Ketone C2. Ketone C2 resonating at 201 ppm has a cross-peak with the nonprotonated C1 at 70 ppm in **Figure 9a**, whose chemical shift and pronounced peak in the HSQC spectrum of **Figure 8** proves an NCq structure. According to **Figure 8e**, this quaternary alkyl C1 is bonded to amide nitrogen resonating at a ^{15}N chemical shift of 122 ppm. In **Figure 9c**, ketone carbons have cross-peaks with aromatic carbon at 138 ppm, which are absent in **Figure 9a** and can therefore not be due to C1 or C2. On this basis, structure Ea can be proposed, where the ketone is bonded to C3, and C3–6 form a pyrrole ring. This accounts for some of the signals near 135 ppm in the spectra of C3 and C6 as shown in **Figures 6h** and **5h**, respectively.

The same structure involving C1 and C2 can be linked to $C3H_2$, according to a broad cross-peak near (200 and 40 ppm) in **Figure 9c**. On the basis of the intensity of the NC1q peak, structures Ea and Eb together account for ca. 4% of all sugar C. It is interesting to note that the similar structures A and E could both be explained in terms of a $C2(OH)_2$ geminal diol intermediate that undergoes water loss.

Furans. The band from 160 to 140 ppm in **Figure 3a** must be assigned to aromatic C bonded to O. Most of them are associated with oxygen-containing aromatic rings, such as furans, in which the two carbons directly linked to oxygen resonate at ~150 ppm, while the carbons two bonds from the oxygen resonate at ~112 ppm. The corresponding cross-peak is clearly seen in the 2D spectrum of **Figure 9c**,**d** (but absent from **Figure 9a**, since glucose C1 and C2 are rarely both incorporated into a furan ring). A distinct cross-peak near (150 and 60 ppm) can be assigned to the bond between the furan ring and OCH_2, which should be assigned to C6, given that this peak is absent from the 2D spectrum of the $^{13}C1-^{13}C2$ sample in **Figure 9a**. Another clear peak at (150 and 15 ppm) can be attributed to $C6H_3$ bonded to the furan ring.

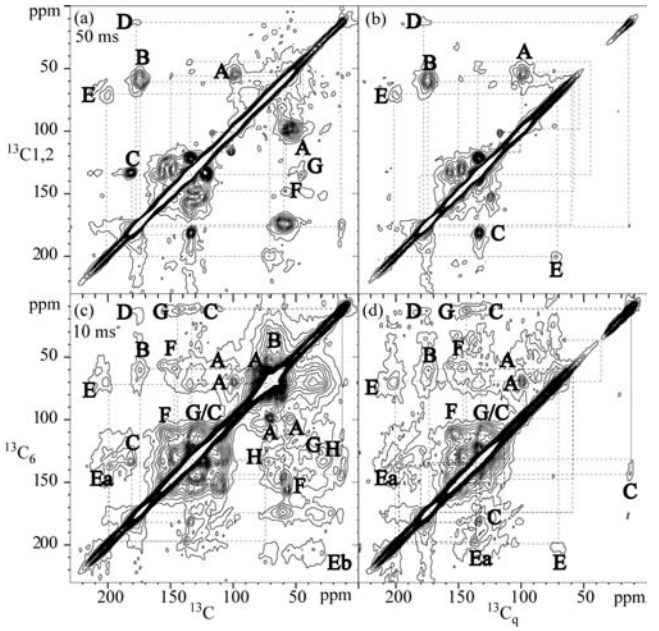

Figure 9. $^{13}C-^{13}C$ spin exchange spectra at 7 kHz MAS. Panels **a** and **b** are for the samples made from 50% diluted glucose-$^{13}C1,2$ reacted with glycine-^{15}N, and panels **c** and **d** for the soluble HMW melanoidins made from glucose-$^{13}C_6$ reacted with glycine-^{15}N. Spectra **b** and **d** show only nonprotonated and methyl carbon signals in the ω_2 (horizontal) dimension, selected by 40 μs of gated decoupling. Prominent cross-peaks are labeled with capital letters matching structures in **Table 1**.

C2 and C4 + C5 contribute comparable nonprotonated carbons resonating at the 150 ± 10 ppm, see **Figure 3c**,**e**, while C4 + C5 and C3 have protonated carbons resonating at 110 ± 5 ppm; however, some of the latter are also in pyrrole rings, being two bonds from N; see **Figure 6h**. In Hodge's scheme, 5-hydroxymethyl-2-furaldehyde was proposed as an important intermediate with C1 forming an aldehyde and C6 staying intact. This kind of furan structure can explain why C2 and C5 are not protonated, while C3 and C4 are. Note, however, that no aldehyde bonded to a furan ring is observed in our sample (while an aldehyde bonded to a pyrrole is clearly detected in **Figure 9**). Thus, the C1 carbon of 5-hydroxymethyl-2-furaldehyde would have to undergo further reactions. Our data strongly suggest that C1 is split off ($C_1 + C_5$ fragmentation), consistent with reactions proposed by Tressl et al. (*35*) since aromatic C2−O (at 150 ppm) shows only weak cross-peaks with alkyl C1 in **Figure 9a**. Therefore, structure F can be proposed. From the fraction of the 162 to 142 ppm band in **Figure 3a** that is from C not bonded to N (see **Figure 7d**), it is estimated that furan rings (and their associated $C6H_2$) account for ca. 11% of total sugar carbons.

Pyrroles and Other N-Containing Heterocycles. The pyrrole ring is one of major structural units of melanoidins considered in the literature. It would typically show resonances around 130 ppm for the C bonded to N, and around 110 ppm for the C two bonds from N. A corresponding cross-peak from this pair of directly bonded carbons is clearly observed in **Figure 9c**,**d** (but absent from **Figure 9a**, since glucose C1 and C2 are rarely both incorporated into a pyrrole ring). The intensity between 116.5 and 104 ppm in **Figure 3d**,**e**, which is due to aromatic C two bonds from N or O as well as from some di-*O*-alkyl C, gives a good estimate of the total pyrrole and furan fractions (~19%, including one associated alkyl C), after correction for di-*O*-alkyl background (see **Figure 7b**). Given 11% furan, pyrroles (including associated alkyl-C6) account for ca. 8% of all glucose C. This is roughly compatible with the ~50% fraction of carbons in this spectral range that are two bonds from N; see **Figure 7d**.

In **Figure 3a**, carbon intensities between 140 and 115 ppm are contributed in similar amounts by most glucose carbons, except for C6. In this chemical shift region, around 85% of C1 and C2 and 9% of C3 are directly bonded to nitrogen, according to **Figures 5d** and **6d**,**h**. **Figure 5h** shows that very little C6 is directly bonded to nitrogen; in the dominant OCH_2 form, it is not even close to nitrogen within two bonds, but as CH_3 and $C-CH_2-C$, it is bonded to pyrrole rings. According to **Figure 7d**, 2/3 of carbons in the 140 to 115 ppm range could be assigned to nitrogen-containing

Table 1. Alkyl and Other Major Structural Fragments Identified in Melanoidins Made from Glucose Reacted with Glycine in a Molar 1:1 Ratio in a Dry Reaction

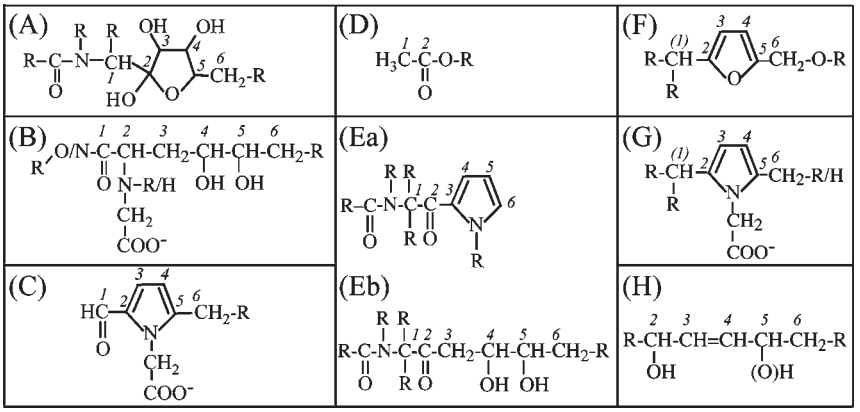

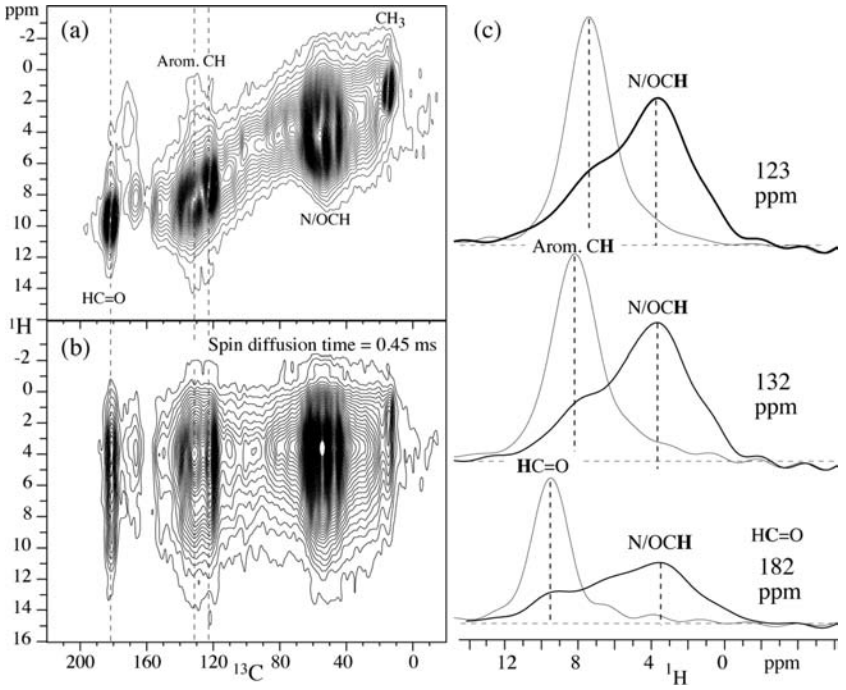

Figure 10. Two-dimensional $^{13}C-^{1}H$ HetCor spectra taken at 10 kHz MAS, with 0.05 ms CP contact time, on soluble HMW melanoidin prepared from glucose-$^{13}C1$ with glycine-^{15}N. (**a**) Without spin diffusion, showing only cross-peaks of directly bonded C−H spin pairs. (**b**) With 0.45 ms of spin diffusion allowing ^{1}H signals of adjacent moieties to be observed. (**c**) ^{1}H spectra obtained as cross-sections taken at ^{13}C chemical shifts of 123, 132, and 182 ppm. Thin lines show cross-sections from panel **a**, and thick lines are from panel **b**.

heteroaromatic compounds, such as pyrrole, imidazolium, or oxazolium rings. According to **Figure 3a**, carbon resonating between 140 and 115 ppm accounts for 19% of all C; thus, about 19% × 2/3 = 12% of all carbons are aromatic and bonded to N. However, the ^{15}N signals downfield from 160 ppm in one-dimensional spectra (*15*, *18*, *20*) and in the HSQC spectra of **Figure 8** show that most C1 and some of the other carbons are involved not in simple pyrrole but in more complex N-containing rings, such as oxazolium and imidazolium. This is confirmed by the analysis of $^{15}N-^{13}C-^{13}C$ spectra, detailed in a forthcoming publication. Nevertheless, the ^{15}N signal of C2 at 150 ppm in **Figure 8c**,**f** and protonated C3 carbons two bonds from N and resonating at 110 ± 5 ppm in **Figure 6h** are good indicators of regular pyrrole rings. According to the ^{15}N spectra of **Figure 8**, imidazolium and oxazolium taken together (and with associated alkyl groups) account for a slightly smaller fraction than the pyrroles, of ca. 6%.

Alkene Structure. Evidence of HC3═C4H alkene is provided by the spectra of C3 and C4 in **Figures 3** and **6**, which exhibit similar fractions (~7%) of protonated sp^2-hybridized carbons resonating near 132 ppm. According to their chemical shifts and the spectra of **Figures 6h** and **7d**, they are not close to N or O in aromatic rings. At the same time, the carbon presumably bonded to C3, that is, C2, is bonded to N and O when it is in aromatic rings. This suggests that the HC3═C4H fragment is not aromatic but an alkene in a structure like H in **Table 1**, which also matches alkene intermediates in the Maillard reaction proposed previously (*4*). Taking background signals into account, this component represents about 6% of all glucose C.

Mixing of Alkyl and Aromatic Units. It could be considered that the alkyl segments are incompletely transformed due to kinetic trapping, for instance, resulting from limited diffusion of the reaction product H_2O from the core of a grain of the reaction mixture. This "core-shell" hypothesis is refuted by the intimate mixing, on the 2 nm scale, of aromatic and *O*-alkyl segments that is demonstrated by $^{1}H-^{13}C$ HetCor NMR with ^{1}H spin diffusion. $^{1}H-^{13}C$ spectra of melanoidin prepared from glucose-$^{13}C1$ and glycine-^{15}N, without and with 0.45 ms of spin diffusion, are plotted as contour plots in **Figure 10a**,**b**, respectively. **Figure 10c** shows the ^{1}H cross-sections at ^{13}C chemical shifts of 123, 132, and 182 ppm from the two spectra superimposed; the dramatic change in the ^{1}H line shapes indicates proximity of the aromatic and HC═O moieties to abundant polar alkyl protons. With a spin diffusion coefficient of ca. 0.5 nm^2/ms, 0.45 ms of spin diffusion equilibrates the ^{1}H magnetization within a sphere of ca. 2 nm diameter. In particular, the HC═O group bonded to a pyrrole ring (see structure C in **Table 1**) essentially equilibrates with alkyl OCH proton magnetization within only 0.45 ms of spin diffusion (see **Figure 10c**, bottom panel).

Synopsis of Structures. The 11 components identified here account for the major peaks in the spectra of the various glucose carbons and for about half of all the glucose carbon in the melanoidin. The other half is probably made up of a variety of minor structural components. For instance, **Figure 3** shows that C2 of glucose accounts for half of the total ketone signal (near 200 ppm), while the other half is contributed as small signals by the other five carbons of glucose.

The absence of a single dominant structure is directly proved by the absence of any peak in the spectrum of $^{13}C1$-labeled melanoidin that accounts for more than 15% of the total intensity. In other words, given that spectral editing (see **Figure 5**) reveals 10 different peaks of fairly similar intensity, there must be at least 10 different structures of significant concentration. Progressively less structural diversity is observed for C2 and C3, see **Figure 6**, with one and two peaks, respectively, of ca. 20% intensity, C4 and C5 with 25% OCH, and C6 with 50% OCH_2. Our results show that melanoidins are structurally more complex than assumed in any previous models. In other words, this structural complexity explains why no simple model of melanoidins has been able to represent their structure in a satisfactory way. A model based mostly on furans and pyrroles (*4*) captures less than half of the melanoidin composition, but models without pyrroles (*12*, *13*) also miss a significant structural component.

At the same time, the structure of our melanoidin is not completely random; our study has shown that certain components are common, while others are rare. For instance, pyridines are insignificant in our sample; their characteristic ^{13}CH or ^{13}C{^{15}N} signals near 160 ppm are observed very weakly only in the spectra of **Figures 5** and **6**. This is consistent with their small concentration in a pyrolysis/mass spectrometry study of a melanoidin produced using the same standard procedure as in our study (*23*).

Supporting Information Available: Contributions of glucose carbons to melanoidins, main features of the alkyl carbons in the glucose:glycine 1:1 melanoidins, and figure of quantitative ^{13}C NMR spectra of insoluble melanoidins. This material is available free of charge via the Internet at http://pubs.acs.org.

LITERATURE CITED

(1) Hodge, J. E. Chemistry of browning reaction in model system. *J. Agric. Food Chem.* **1953**, *1*, 926.

(2) Ledl, F.; Schleicher, E. New aspects of the Maillard reaction in foods and in the human body. *Angew. Chem. Int. Engl. Ed.* **1990**, *29*, 565.

(3) Tressl, R.; Kersten, E.; Rewicki, D. Formation of Pyrroles, 2-Pyrrolidones, and Pyridones by Heating of 4-Aminobutyric Acid and Reducing Sugars. *J. Agric. Food Chem.* **1993**, *41*, 2125.

(4) Tressl, R.; Wondrak, G. T.; Garbe, L. A. Pentoses and Hexoses as Sources of New Melanoidin-like Maillard Polymers. *J. Agric. Food Chem.* **1998**, *46*, 1765.

(5) Nursten, H. *The Maillard Reaction: Chemistry, Biochemistry and Implications*; Royal Society of Chemistry: Cambridge, United Kingdom, 2005.

(6) O'Brien, J.; Nursten, H. E.; Crabbe, M. J.; Ames, J. M. *The Maillard Reaction in Foods and Medicine*; RSC Publishing: Cambridge, United Kingdom, 1998.

(7) Ikan, R. *The Maillard Reaction Consequences for the Chemical and Life Sciences*.; John Wiley & Sons Ltd.: New York, 1996.

(8) Ames, J. M.; Bailey, R. G.; Mann, J. Analysis of furanone, pyranone, and new heterocyclic colored compounds from sugar-glycine model Maillard systems. *J. Agric. Food Chem.* **1999**, *47*, 438.

(9) Hofmann, T. Characterization of the chemical structure of novel colored Maillard reaction products from furan-2-carboxaldehyde and amino acids. *J. Agric. Food Chem.* **1998**, *46*, 932.

(10) Amrani-Hemaimi, M.; Cerny, C.; Fay, L. B. Mechanisms of formation of alkylpyrazines in the Maillard reaction. *J. Agric. Food Chem.* **1995**, *43*, 2818.

(11) Hofmann, T.; Ames, J.; Krome, K.; Faist, V. Determination of the molecular weight distribution of nonenzymatic browning products formed by roasting of glucose and glycine and studies on their effects on NADPH-cytochrome c-reductase and glutathione-S-transferase in Caco-2 cells. *Nahrung/Food* **2001**, *45*, 189.

(12) Cämmerer, B.; Kroh, L. W. Investigation of the influence of reaction conditions on the elementary composition of melanoidins. *Food Chem.* **1995**, *53*, 55.

(13) Kato, H.; Tsuchida, H. Estimation of melanoidin structure by pyrolysis and oxidation. *Progr. Food Nutr. Sci.* **1981**, *5*, 147.

(14) Yaylayan, V. A.; Kaminsky, E. Isolation and structural analysis of Maillard polymers: Caramel and melanoidin formation in glycine/glucose model system. *Food Chem.* **1998**, *63*, 25.

(15) Benzing-Purdie, L.; Ripmeester, J. A.; Preston, C. M. Elucidation of the nitrogen forms in melanoidins and humic acid by nitrogen-15 cross polarization-magic angle spinning nuclear magnetic resonance spectroscopy. *J. Agric. Food Chem.* **1983**, *31*, 913.

(16) Benzing-Purdie, L.; Ripmeester, J. A.; Ratcliffe, C. I. Effects of Temperature on Maillard Reaction Products. *J. Agric. Food Chem.* **1985**, *33*, 31.

(17) Ikan, R.; Ioselis, P.; Rubinsztain, Y.; Aizenshtat, Z.; Pugmire, R.; Anderson, L. L.; Woolfenden, W. R. Carbon-13 cross polarized magic angle samples spinning nuclear magnetic resonance of melanoidins. *Org. Geochem.* **1986**, *9*, 199.

(18) Hayase, F.; Kim, S. B.; Kato, H. Analyses of the chemical structures of melanoidins by ^{13}C NMR, ^{13}C and ^{15}N CP-MAS NMR spectrometry. *Agric. Biol. Chem.* **1986**, *50*, 1951.

(19) Benzing-Purdie, L.; Ripmeester, J. A. Maillard-reaction: Investigation of the chemical structure of melanoidins synthesized from D-xylose/glycine using ^{13}C- and ^{15}N-specifically labeled reactants. *J. Carbohydr. Chem.* **1987**, *6*, 87.

(20) Fang, X.; Schmidt-Rohr, K. Fate of the Amino Acid in Glucose-Glycine Melanoidins Investigated by Solid-State Nuclear Magnetic Resonance (NMR). *J. Agric. Food Chem.* **2009**, *57*, 10701.

(21) Ames, J. M. EU COST action 919: melanoidins in food and health. *Int. Congr. Ser.* **2002**, *1245*, 389.

(22) Abbaspour Tehrani, K.; Kersiene, M.; Adams, A.; Venskutonis, R.; De Kimpe, N. Thermal Degradation Studies of Glucose/Glycine Melanoidins. *J. Agric. Food Chem.* **2002**, *50*, 4062.

(23) Adams, A.; Abbaspour Tehrani, K.; Kersiene, M.; Venskutonis, R.; De Kimpe, N. Characterization of Model Melanoidins by the Thermal Degradation Profile. *J. Agric. Food Chem.* **2003**, *51*, 4338.

(24) Dixon, W. T. Spinning-sideband-free and spinning-sideband-only NMR spectra in spinning samples. *J. Chem. Phys.* **1982**, *77*, 1800.

(25) Mao, J.-D.; Hu, W.-G.; Schmidt-Rohr, K.; Davies, G.; Ghabbour, E. A.; Xing, B. Quantitative characterization of humic substances by solid-state carbon-13 nuclear magnetic resonance. *Soil Sci. Soc. Am. J.* **2000**, *64*, 873.

(26) Schmidt-Rohr, K.; Mao, J. D. Efficient CH-Group Selection and Identification in ^{13}C Solid-State NMR by Dipolar DEPT and ^{1}H Chemical-Shift Filtering. *J. Am. Chem. Soc.* **2002**, *124*, 13938.

(27) Mao, J.-D.; Schmidt-Rohr, K. Methylene spectral editing in solid-state ^{13}C NMR by three-spin coherence selection. *J. Magn. Reson.* **2005**, *176*, 1.

(28) Mao, J.-D.; Schmidt-Rohr, K. Accurate Quantification of Aromaticity and Nonprotonated Aromatic Carbon Fraction in Natural Organic Matter by ^{13}C Solid-State Nuclear Magnetic Resonance. *Environ. Sci. Technol.* **2004**, *38*, 2680.

(29) Chan, J. C. C.; Tycko, R. Recoupling of chemical shift anisotropies in solid-state NMR under high-speed magic-angle spinning and in uniformly ^{13}C-labeled Systems. *J. Chem. Phys.* **2003**, *118*, 8378.

(30) Mao, J.-D.; Schmidt-Rohr, K. Separation of Aromatic-carbon ^{13}C NMR Signals from Di-oxygenated Alkyl Bands by a Chemical-shift-anisotropy Filter. *Solid State Nucl. Magn. Reson.* **2004**, *26*, 36.

(31) Yao, X.-L.; Schmidt-Rohr, K.; Hong, M. Medium- and Long-Distance ^{1}H−^{13}C Heteronuclear Correlation NMR in Solids. *J. Magn. Reson.* **2001**, *149*, 139.

(32) Bodenhausen, G.; Ruben, D. J. Natural abundance nitrogen-15 NMR by enhanced heteronuclear spectroscopy. *Chem. Phys. Lett.* **1980**, *69*, 185.

(33) Geen, H.; Bodenhausen, G. Pure absorption-mode chemical exchange NMR spectroscopy with suppression of spinning sidebands in a slowly rotating solid. *J. Chem. Phys.* **1992**, *97*, 2928.

(34) Tressl, R.; Helak, B.; Kersten, E.; Rewicki, D. Formation of Proline- and Hydroxyproline-Specific Maillard Products from [l-^{13}C]Glucose. *J. Agric. Food Chem.* **1993**, *41*, 547.

(35) Tressl, R.; Nittka, C.; Kersten, E. Formation of Isoleucine-Specific Maillard Products from [l-^{13}C]-D-Glucose and [l-^{13}C]-D-Fructose. *J. Agric. Food Chem.* **1995**, *43*, 1163.

Received for review July 27, 2010. Revised manuscript received November 13, 2010. Accepted November 20, 2010. This work was supported by the National Science Foundation (Grant CHE-0138117).